Acta Crystallographica Section F
Structural Biology and Crystallization Communications
ISSN 1744-3091

Structure of an *Escherichia coli* *N*-acetyl-D-neuraminic acid lyase mutant, E192N, in complex with pyruvate at 1.45 Å resolution

Ivan Campeotto,[a] Stephen B. Carr,[a,b] Chi H. Trinh,[a] Adam S. Nelson,[a] Alan Berry,[a] Simon E. V. Phillips[a,b] and Arwen R. Pearson[a]*

[a]Astbury Centre for Structural Molecular Biology, University of Leeds, Leeds LS2 9JT, England, and [b]Research Complex at Harwell, Rutherford Appleton Laboratory, Harwell Science and Innovation Campus, Oxon OX11 0FA, England

Correspondence e-mail: a.r.pearson@leeds.ac.uk

Received 6 July 2009
Accepted 15 September 2009

PDB Reference: *N*-acetyl-D-neuraminic acid lyase, 2wkj, r2wkjsf.

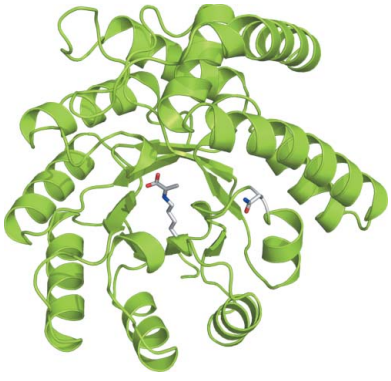

The structure of a mutant variant of *Escherichia coli* *N*-acetyl-D-neuraminic acid lyase (NAL), E192N, in complex with pyruvate has been determined in a new crystal form. It crystallized in space group $P2_12_12_1$, with unit-cell parameters $a = 78.3$, $b = 108.5$, $c = 148.3$ Å. Pyruvate has been trapped in the active site as a Schiff base with the catalytic lysine (Lys165) without the need for reduction. Unlike the previously published crystallization conditions for the wild-type enzyme, in which a mother-liquor-derived sulfate ion is strongly bound in the catalytic pocket, the low-salt conditions described here will facilitate the determination of further *E. coli* NAL structures in complex with other active-site ligands.

1. Introduction

N-Acetyl-D-neuraminic acid lyase (NAL; EC 4.1.3.3) catalyses the reversible aldol condensation of pyruvate and *N*-acetyl-D-mannosamine to yield *N*-acetyl-D-neuraminic acid (Brunetti *et al.*, 1962; Schauer *et al.*, 1999). NAL belongs to the aldolase family, which can be subdivided into two classes on the basis of the reaction mechanism. In class I aldolases, including NAL, the reaction proceeds through the formation of a Schiff base between a protein lysine residue and the substrate pyruvate, whereas in class II aldolases the intermediates are stabilized by a metal cofactor (*e.g.* Zn^{+}) (Plater *et al.*, 1999). Many structures of class I aldolases have been reported and all share the same TIM-barrel fold (Izard *et al.*, 1994; Wymer *et al.*, 2001; Theodossis *et al.*, 2004; Pauluhn *et al.*, 2008). The structure of NAL from *Escherichia coli* has previously been determined in space group $P3_221$ crystallized from a solution containing saturated ammonium sulfate (Izard *et al.*, 1994). The presence of a sulfate ion strongly bound in the catalytic pocket of this structure has been considered to be the likely cause of the failure of substrate-soaking experiments. Crystals of a mutant *E. coli* NAL from low-salt conditions have been reported in complex with the inhibitor β-hydroxypyruvate (Joerger *et al.*, 2003), but no substrate-complex structures are available. In contrast, NAL from *Haemophilus influenzae* crystallizes readily under low-salt conditions and several complexes with inhibitors or substrate analogues have been reported (Barbosa *et al.*, 2000), although the pyruvate Schiff-base complex could only be trapped after reduction by sodium borohydride (Izard *et al.*, 1994).

A range of analogues of *N*-acetyl-D-neuraminic acid are well established drugs for the treatment of influenza, targeting the sialidase (von Itzstein, 2007). Some potent inhibitors of influenza A sialidase have been discovered in which the glycerol side chain of *N*-acetyl-D-neuraminic acid has been replaced by a dialkylaminocarbonyl substituent (Smith *et al.*, 1998; Taylor *et al.*, 1998). Unfortunately, these modified ligands may not readily be prepared using wild-type *E. coli* NAL as the catalyst and require complex chemical synthesis. The enzyme has therefore been subjected to directed evolution (Williams *et al.*, 2005) in order to broaden its substrate specificity. This programme resulted in the discovery of the mutant variant E192N, which has a sixfold higher specificity (k_{cat}/K_m) for dipropylaminocarbonyl-substituted derivatives than wild-type NAL

Table 1
Data-collection and refinement statistics.

Values in parentheses are for the outermost shell of the resolution range.

Data collection	
Space group	$P2_12_12_1$
Unit-cell parameters (Å)	a = 78.3, b = 108.5, c = 148.3
Resolution (Å)	63.41–1.45 (1.53–1.45)
R_{merge}†	0.077 (0.375)
$R_{p.i.m.}$‡	0.036 (0.172)
$\langle I\rangle/\mathrm{sd}\langle I\rangle$	11.6 (3.4)
Completeness (%)	96.2 (89.5)
Redundancy	5.1 (4.9)
Refinement	
No. of reflections	1095072 (138933)
No. of unique reflections	213226 (28642)
R_{work}§	0.167 (0.280)
R_{free}	0.189 (0.290)
No. of atoms	10677
Protein	9336
Ligands	34
Water	1307
Average B factors (Å^2)	
Protein	14.4
Covalently bound pyruvate	10.8
Noncovalently bound pyruvate	28.7
PEG 400	50.0
Waters	16.5
R.m.s. deviations¶	
Bond lengths (Å)	0.012
Bond angles (°)	1.346
Ramachandran statistics†† (%)	
Most favoured	100
Outliers	0
PDB code	2wkj

† $R_{merge} = \sum_{hkl}\sum_i |I_i(hkl) - \langle I(hkl)\rangle|/\sum_{hkl}\sum_i I_i(hkl)$. ‡ $R_{p.i.m.} = \sum_{hkl}[1/(N-1)]^{1/2} \times \sum_i |I_i(hkl) - \langle I(hkl)\rangle|/\sum_{hkl}\sum_i I_i(hkl)$. § The crystallographic R factor was calculated as $\sum_{hkl}\big||F_{obs}| - |F_{calc}|\big|/\sum_{hkl}|F_{obs}|$, with 5% of reflections set aside randomly for calculation of R_{free}. ¶ Based on the ideal geometry values of Engh & Huber (1991). †† Ramachandran analysis using the program *MolProbity* (Davis *et al.*, 2007).

has for its natural substrate sialic acid (Williams *et al.*, 2005). We are pursuing X-ray structures of complexes of this NAL variant with substrates and inhibitors in order to identify the structural basis of the improved specificity. Here, we report a new crystal form of *E. coli* NAL obtained under low-salt conditions, which will allow us to carry out substrate-soaking experiments. We present the high-resolution structure (1.45 Å) of the variant E192N–pyruvate complex obtained by cocrystallization with pyruvate without the need for trapping by sodium borohydride reduction.

2. Experimental

The *E. coli* NAL variant E192N was isolated and purified as previously described (Williams *et al.*, 2005). The protein was concentrated to 10 mg ml^{-1} and incubated for 1 h at 310 K with 100 m*M* sodium pyruvate before setting up crystallization trials.

Initial sitting-drop trials were performed by screening different commercial conditions from Hampton Research (Index, SaltRx, Crystal Screen and MembFac) and Emerald BioSystems (Wizard I and II) using an Oryx 6 robot (Douglas Instruments). The best crystals grew from 100 m*M* Tris–HCl pH 8.2, 200 m*M* ammonium acetate, 18% PEG 3350. Plate-shaped crystals appeared after 10 d at 277 K. Data were collected to a resolution of 1.45 Å from a single crystal at 100 K at the Diamond Synchrotron Light Source (station I04), were indexed using *MOSFLM* (Leslie, 2006) and were scaled and merged using *SCALA* (Evans, 2006) (Table 1). 5% of the reflections were excluded from the refinement and constituted the R_{free} set. The structure was solved by molecular replacement using *Phaser* (McCoy, 2007) with the structure of the *E. coli* NAL wild-type protein as the search model (PDB code 1nal). Refinement was carried out with *REFMAC* (Murshudov *et al.*, 1997). Stereochemical restraints for the ligand pyruvate bound to Lys165 were obtained from *PRODRG* (http://davapc1.bioch.dundee.ac.uk/prodrg/index.html), while TLS refinement was applied following determination of TLS

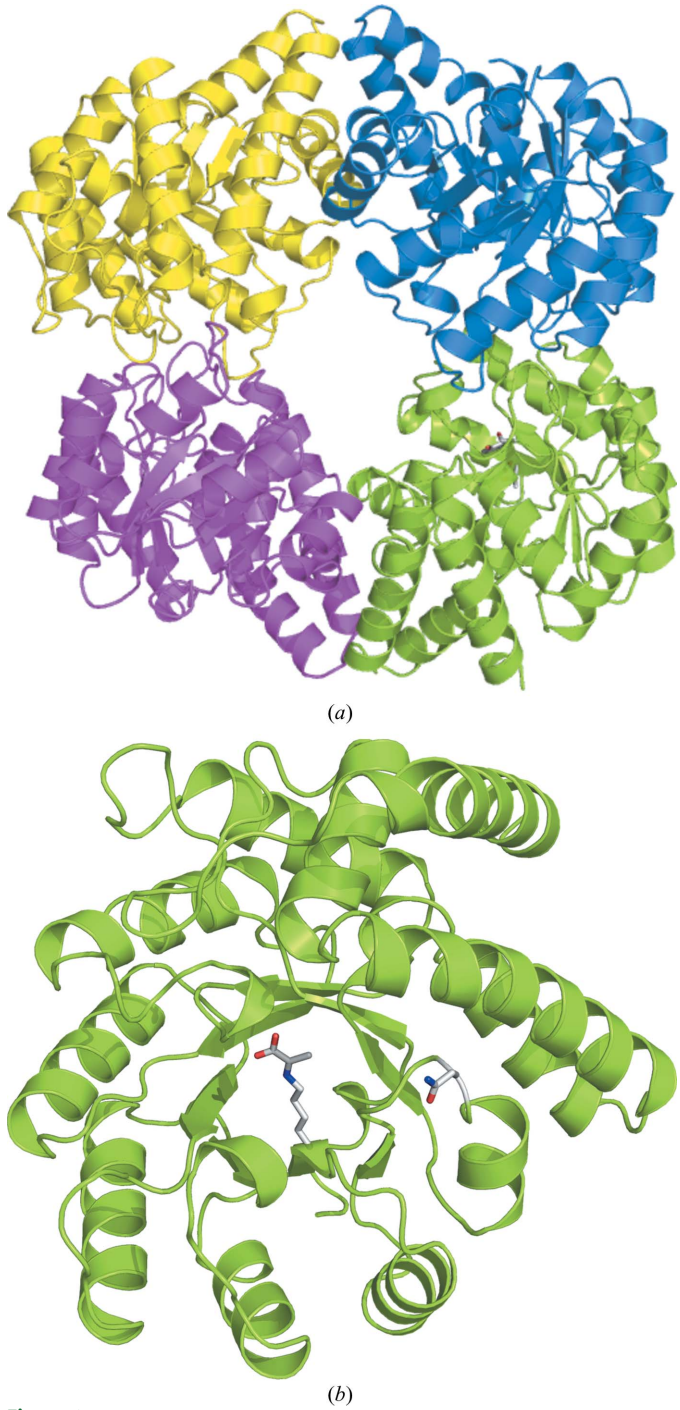

Figure 1
(*a*) Overall structure of the NAL variant E192N homotetramer showing each chain of the NAL variant E192N as a coloured ribbon. In the green-coloured monomer both the Schiff-base complex between Lys165 and pyruvate and the mutated residue E192N are shown as sticks coloured by atom type. (*b*) View of a single NAL monomer, showing the location of the lysine–pyruvate Schiff base and the E192N mutation within the α/β barrel. This figure was generated using *PyMOL* v.0.99 (DeLano, 2002).

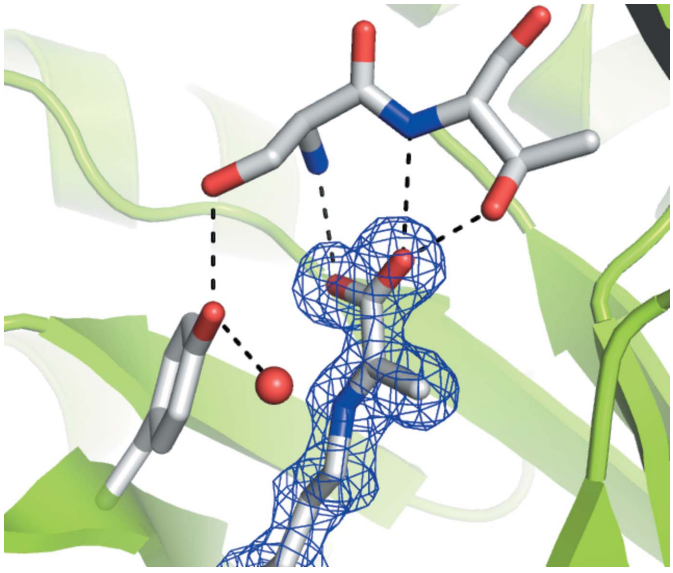

Figure 2
Electron density for the Schiff base between Lys165 and pyruvate. The planarity of the $2F_o - F_c$ map (contoured at 1.0 r.m.s.) is consistent with the formation of a Schiff base between Lys165 and pyruvate. The hydrogen-bond network between pyruvate and Thr48 and Ser47 and between Tyr137, Ser47 and a water is well conserved in all members of the NAL family.

domains using the *TLSMD* server (http://skuld.bmsc.washington.edu/~tlsmd/). Superposition of structures and calculation of their r.m.s. deviation were performed with *LSQKAB* (Collaborative Computational Project, Number 4, 1994). Water molecules were added in *Coot* (Emsley & Cowtan, 2004) for peaks over 3.0σ in the $F_o - F_c$ map and structure validation was carried out with *MolProbity* (Davis *et al.*, 2007).

3. Results and discussion

E192N NAL in space group $P2_12_12_1$ has one noncrystallographic tetramer per asymmetric unit, with a very similar structure to that of the wild-type enzyme (PDB code 1nal) determined in space group $P3_221$ (Fig. 1). The r.m.s.d. between these structures is only 0.5 Å for all atoms, despite the difference in space group and crystallization conditions. The structure is also very similar to that of the L142R β-hydroxypyruvate inhibitor-complex structure (PDB code 1hl2; 0.8 Å r.m.s.d. for all atoms; Joerger *et al.*, 2003), which was determined under different low-salt conditions in space group $P2_1$ (100 m*M* sodium acetate pH 4.6 and 8% PEG 4000). For the first time for *E. coli* NAL we were able to trap the Schiff-base complex between pyruvate and Lys165 without the need for reduction with sodium borohydride. Schiff-base formation is confirmed by the planarity of the electron-density map for the conjugated pyruvate (Fig. 2). The hydrogen-bond network between pyruvate and Ser47 and Thr48, and between Tyr137 and Ser47 and a water (here water 48) is well conserved in all the NAL family members (Fig. 2). One additional noncovalently bound pyruvate molecule is present in the catalytic pocket of subunits *C* and *D*, probably owing to the high concentration of sodium pyruvate in the crystallization buffer. One molecule of cryoprotecting agent PEG 400 is also present in both chain *A* and chain *C*, lying on the twofold axis. We have also been able to obtain diffracting crystals of wild-type *E. coli* NAL under the same conditions (data not shown). These new low-salt crystallization conditions for *E. coli* NAL are particularly exciting as they will allow ligand- and inhibitor-soaking studies that were not possible under the previously published high-salt crystallization conditions. These will enable us to probe the origin of the broadened substrate specificity of the E192N variant.

IC is supported by a Wellcome Trust PhD Studentship. ARP is supported by a RCUK Fellowship. This work was supported by the BBSRC (BB/E000622/1). We thank the MX beamline staff at Diamond Light Source for assistance with data collection.

References

Barbosa, J. A., Smith, B. J., DeGori, R., Ooi, H. C., Marcuccio, S. M., Campi, E. M., Jackson, W. R., Brossmer, R., Sommer, M. & Lawrence, M. C. (2000). *J. Mol. Biol.* **303**, 405–421.
Brunetti, P., Jourdian, G. W. & Roseman, S. (1962). *J. Biol. Chem.* **237**, 2447–2453.
Collaborative Computational Project, Number 4 (1994). *Acta Cryst.* D**50**, 760–763.
Davis, I. W., Leaver-Fay, A., Chen, V. B., Block, J. N., Kapral, G. J., Wang, X., Murray, L. W., Arendall, W. B. III, Snoeyink, J., Richardson, J. S. & Richardson, D. C. (2007). *Nucleic Acids Res.* **35**, W375–W383.
DeLano, W. L. (2002). *The PyMOL Molecular Graphics System.* http://www.pymol.org.
Emsley, P. & Cowtan, K. (2004). *Acta Cryst.* D**60**, 2126–2132.
Engh, R. A. & Huber, R. (1991). *Acta Cryst.* A**47**, 392–400.
Evans, P. (2006). *Acta Cryst.* D**62**, 72–82.
Itzstein, M. von (2007). *Nature Rev. Drug Discov.* **6**, 967–974.
Izard, T., Lawrence, M. C., Malby, R. L., Lilley, G. G. & Colman, P. M. (1994). *Structure*, **2**, 361–369.
Joerger, A. C., Mayer, S. & Fersht, A. R. (2003). *Proc. Natl Acad. Sci. USA*, **100**, 5694–5699.
Leslie, A. G. W. (2006). *Acta Cryst.* D**62**, 48–57.
McCoy, A. J. (2007). *Acta Cryst.* D**63**, 32–41.
Murshudov, G. N., Vagin, A. A. & Dodson, E. J. (1997). *Acta Cryst.* D**53**, 240–255.
Pauluhn, A., Ahmed, H., Lorentzen, E., Buchinger, S., Schomburg, D., Siebers, B. & Pohl, E. (2008). *Proteins*, **72**, 35–43.
Plater, A. R., Zgiby, S. M., Thomson, G. J., Qamar, S., Wharton, C. W. & Berry, A. (1999). *J. Mol. Biol.* **285**, 843–855.
Schauer, R., Sommer, U., Krueger, D., van Unen, H. & Traving, C. (1999). *Biosci. Rep.* **19**, 373–383.
Smith, P. W. *et al.* (1998). *J. Med. Chem.* **41**, 787–797.
Taylor, N. R., Cleasby, A., Singh, O., Skarzynski, T., Wonacott, A. J., Smith, P. W., Sollis, S. L., Howes, P. D., Cherry, P. C., Bethell, R., Colman, P. & Varghese, J. (1998). *J. Med. Chem.* **41**, 798–807.
Theodossis, A., Walden, H., Westwick, E. J., Connaris, H., Lamble, H. J., Hough, D. W., Danson, M. J. & Taylor, G. L. (2004). *J. Biol. Chem.* **279**, 43886–43892.
Williams, G. J., Woodhall, T., Nelson, A. & Berry, A. (2005). *Protein Eng. Des. Sel.* **18**, 239–246.
Wymer, N., Buchanan, L. V., Henderson, A., Mehta, N., Botting, C. H., Pocivasvsek, L., Fierke, C. A., Toon, E. J. & Naismith, J. H. (2001). *Structure*, **9**, 1–9.